

Relative light sensitivities of four retinal hemi-fields for suppressing the synthesis of melatonin at night

Mark S. Rea^{*}, Rohan Nagare, Mariana G. Figueiro

Light and Health Research Center, Department of Population Health Science and Policy, Icahn School of Medicine at Mount Sinai, New York, NY, USA

ARTICLE INFO

Keywords:

Circadian phototransduction
Monocular
Melatonin suppression
Blue light
Nasal retina

ABSTRACT

The magnitude of the stimulus to the biological clock will depend upon the distribution of circadian phototransduction circuits across the retinae and the spatial distribution of luminous stimuli in the environment. The present study compared nocturnal melatonin suppression for light exposures to the superior, inferior, nasal, and temporal retina in one eye independent of shading from the brow and the nose. The stimulus was a 40° diameter luminous disc, half of which was blue light (LED, $\lambda_{\text{peak}} = 470$ nm) and the other amber light (LED, $\lambda_{\text{peak}} = 590$ nm). Experimentally, the orientation of the bipartite disc was rotated to each of the four cardinal points of the visual field. A full, 40° blue disc was also employed by replacing the amber half-disc with another blue half-disc. The blue full- and half-discs always produced 100 photopic lx at the cornea. As hypothesized, nocturnal melatonin suppression was statistically greatest when the blue half-disc was delivered to the nasal hemi-field (35%); the other three hemi-fields were equally affected by the blue half-disc ($\approx 20\%$). Melatonin suppression for the full-disc was 24%, which was not statistically different than the average suppression for the four hemi-fields of 27%.

1. Introduction

The purpose of the present study was to help resolve a discrepancy in the psychophysical literature about the spatial sensitivity of the retina to circadian-effective light. Helping to resolve this issue has implications both for clinical applications (Where should a light box be placed for maximum efficacy?) and for architectural applications (Is it more effective to deliver ambient room lighting from the ceiling or from a window?).

Two psychophysical reports suggest that the nasal retina is most sensitive to circadian effective light (Rüger et al., 2005; Visser et al., 1999) while others report greater sensitivity in the inferior retina (Glickman et al., 2003; Lasko et al., 1999) and one report suggests that the inferior retina is less sensitive than on-axis exposures (Gaddy et al., 1992).

The neuroanatomy of the retina suggests that the macular region of the retina and the nasal field should be more sensitive to circadian effective light than the rest of the retina due to the high density of intrinsically photosensitive retinal ganglion cell (ipRGC) cell bodies in

the macular region and due to the ipRGC axons linking the macular region of the retina to the optic disc. The highest density of ganglion cell bodies in the human retina, including those of the ipRGCs (Esquiva et al., 2017; La Morgia et al., 2010), form a concentric ring approximately 15–20° in diameter (Kolb et al., 2020) in the macula surrounding the central fovea. Thus, consistent with the report from Gaddy et al. (1992), the macula should be more sensitive to circadian-effective light than the inferior retina. The axons from the macular ganglion neurons form the dense, papillomacular bundle before exiting the eye through the optic disc to reach the suprachiasmatic nuclei (SCN). It is well established that the photopigment melanopsin is present throughout the dendrites, cell bodies and axons of the ipRGCs (e.g., Esquiva et al. (2017)). Therefore, the high-density ipRGC axons in the papillomacular bundle should hypothetically provide, in addition to the radially symmetric macula, an asymmetric photosensitive field to circadian effective light in the near nasal retina ($< 20^\circ$). This neuroanatomical evidence is consistent with the findings of Rüger et al. (2005) and Visser et al. (1999).

In the design of the present experiment, it was necessary to control

Abbreviations: α -opic, alpha-opic; ANOVA, analysis of variance; CL_A, circadian light; CS, circadian stimulus; EML, equivalent melanopic lux; LED, light-emitting diode; λ_{peak} , peak wavelength; RGB, red, green, blue.

^{*} Corresponding author. Icahn School of Medicine at Mount Sinai, 1425 Madison Avenue, 2nd Floor, New York, NY, 10029, USA.

E-mail addresses: mark.rea@mountsinai.org (M.S. Rea), rohan.nagare@mountsinai.org (R. Nagare), mariana.figueiro@mountsinai.org (M.G. Figueiro).

<https://doi.org/10.1016/j.nbscr.2021.100066>

Received 11 March 2021; Received in revised form 9 April 2021; Accepted 12 April 2021

Available online 18 April 2021

2451-9944/© 2021 The Authors.

Published by Elsevier Inc.

This is an open access article under the CC BY-NC-ND license

(<http://creativecommons.org/licenses/by-nc-nd/4.0/>).

for the optics of the eye and to provide participants with luminous stimuli that varied only in terms of the spatial distribution of circadian-effective light on the retina. To control for the distribution of light entering the eye (Kooijman, 1983; Pflibsen et al., 1988; Van Derlofske et al., 2002), participants viewed a dynamic fixation point monocularly while a luminous circular field comprised of a circadian-effective (blue) half-field and a circadian-ineffective (amber) half-field was presented. The spatial extent of the entire luminous field (amber and blue) was small enough (40° diameter) to avoid shadowing from the participant's nose or brow.

To differentially stimulate the circadian phototransduction processes in four retinal hemi-fields while maintaining constant, overall retinal stimulation, the circular luminous field was rotated about its central axis (the fixation point) so that the blue half-field was centered on one of the four cardinal directions of the visual field, up, down, left, and right. Thus, the amounts and spectra of light entering the eye were always constant, but the circadian phototransduction mechanisms in the four retinal hemi-fields were differentially stimulated. By this method it was possible to assess the relative effectiveness of circadian phototransduction to light presented in the superior, inferior, nasal, and temporal fields without optical artefacts and with minimal differences in local adaptation across the retina. With regard to this latter point, rods participate in setting the threshold for circadian effective light (Rea et al., 2005, 2021a,b). Because the amber half-field was bright enough to stimulate cone photoreceptors, they would, in turn, suppress possible spatially-dependent rod-intrusion artefacts from an adjacent dark half-field, thereby permitting direct assessment of the circadian phototransduction circuits response to the blue half-field. Although rod-intrusion from the dark surround was possible, it was constant for all stimulus conditions.

As a positive control, the orange half-field was replaced with a blue half-field such that the luminous stimulus was a circular field comprised of blue light producing the same total irradiance at the eye as each of the blue half-fields. As a negative, dark control, the orange and blue fields were extinguished. In both control conditions, as with the experimental conditions, participants maintained fixation for a total of 1 h. Saliva melatonin was sampled at three time points, at the beginning of a session and following 30 min and 60 min. Nocturnal melatonin suppression relative to the normalized dark control at the same time point was used as the outcome measure. This outcome measure, nocturnal melatonin suppression, obviates the large inter-subject variability in absolute melatonin concentrations during the night (e.g., Burgess and Fogg (2008)) thereby enabling us to evaluate the relative sensitivity of the four retinal hemi-fields in our counterbalanced, within-subjects experimental design. It should also be noted that melatonin suppression is an ideal measure of circadian-effective light for two reasons. First, melatonin suppression is dose-dependent, exhibiting a graded response to variations in the spectrum, amount, and duration of light exposure on the retina. Second, the pineal gland that synthesizes melatonin at night receives most, if not all, of its light-dependent stimulation from the SCN which, in turn, has received its light-dependent input from the circadian-phototransduction mechanisms in the retina (Baver et al., 2008; Fernandez et al., 2016; Kriegsfeld et al., 2004; Rea et al., 2021a, 2021b; Rosenwasser and Turek, 2015).

Based upon the neuroanatomy of the retina, and consistent with psychophysical findings from Rüger et al. (2005) and Visser et al. (1999), it was hypothesized that circadian-effective light exposure to the nasal hemi-field would be more effective for suppressing nocturnal melatonin production than the temporal, the superior, and the inferior hemi-fields.

2. Material and methods

2.1. Participant selection

Potential participants were recruited for the study via personal

referrals, word of mouth, Rensselaer Polytechnic Institute's social media platform, and lists of participants from previous studies. Everyone was screened for major health problems such as bipolar disorder, seasonal depression, cardiovascular disease, diabetes, and high blood pressure. Individuals were excluded from participation if they were taking over-the-counter melatonin or prescription medications such as blood pressure medicine, antidepressants, sleep medicine, or beta-blockers. Those reporting eye diseases such as cataracts, glaucoma, and macular degeneration were also excluded. No one was permitted to participate in the study if they planned to undertake transmeridian travel over the course of the study. Potential participants who were identified by the study team as having colour vision deficiency according to Ishihara colour blindness tests (Ishihara, 1960) were excluded. Sixteen adult participants (10 females; mean age = 35.1 years [SD 13.2]) were selected. None in the final pool of participants was an extreme lark (early person) or extreme owl (late person); Munich Chronotype Questionnaire score mean of 3.1 (SD 1.5). (Roenneberg et al., 2003).

To maintain stable entrainment, everyone in the final pool of participants was required to follow a regular sleep-wake schedule every weekday of the study, including the weekdays leading up to the first experimental session, with bedtimes no later than 23:00 and wake times no later than 07:30. Given that all of the participants were full-time, daytime workers, their sleep schedules were presumed to be regular on week nights throughout the duration of the study. Participants were requested to refrain from caffeine and alcohol consumption 12 h prior to the beginning of each experimental session, and compliance was verified based upon verbal reports prior to each session. As a note, most of the participants in the present had served in previous studies in our laboratory, consistently demonstrating compliance with our instructions. Therefore we felt it unnecessary to independently verify their verbal assurance for compliance.

This study conformed to the Code of Federal Regulations (CFR) document Protection of Human Subjects, 45 CFR 46, (2018), and international ethical standards (Portaluppi et al., 2010). It was reviewed, approved, and monitored by Rensselaer Polytechnic Institute's Institutional Review Board. Informed consent was obtained from all study participants.

2.2. Experimental conditions and apparatus

The 6-week study, conducted on Friday nights at the Lighting Research Centre's laboratory in Troy, NY, from October 11, 2019 to November 22, 2019, employed a within-subjects experimental design to minimize uncontrolled differences among individuals. To manage the experimental sessions more efficiently, the participants were arbitrarily divided into groups to counterbalance the experimental conditions (three groups of two, two groups of three, and one group of four participants); each group was exposed to a different experimental condition per session.

On each of the six study nights participants were exposed to a different experimental condition (including the dark control), as illustrated in Fig. 1. Fig. 2 illustrates the apparatus. Spectral irradiance measurements of the blue and amber sources were performed using a spectrometer (Model USB650, Ocean Optics, Winter Park, FL, USA); their relative spectral power distributions are shown in Fig. 3.

While viewing the apparatus during an experimental session, participants placed their chin in a rigid rest and their non-dominant eye was covered with an opaque eye patch. During each experimental condition participants viewed the apparatus, including the dark control, monocularly with their dominant eye. For the fixed viewing distance of 20.5 cm (10 in), the entire luminous disc subtended a visual angle of 40°. To ensure the appropriate regions of the retina was illuminated, participants were requested to view the small, luminous fixation point at the centre of the display. Light for the small fixation point (Fig. 2) was produced by a RGB LED (Inolux, HV-5RGB60) at the end of a narrow tube (diameter = 2.1 mm). Participants had to align their gaze along the

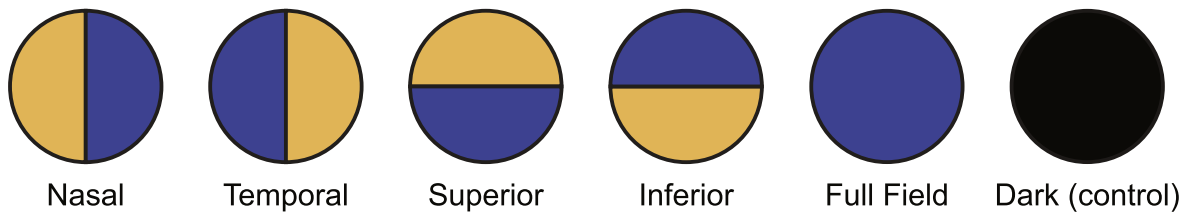


Fig. 1. The five experimental stimulus conditions and the dark control. All six experimental conditions were comprised of a 40° diameter circular field at the participant’s eye. Half of each bipartite field was illuminated with a narrowband blue LED light source ($\lambda_{\text{peak}} = 470 \text{ nm}$) while the other half was illuminated with a phosphor converted amber LED light source ($\lambda_{\text{peak}} = 590 \text{ nm}$). Alone, the blue half-field delivered a CS = 0.60 at the cornea (100 lx), whereas the amber half-field delivered a CS < 0.01 (30 lx). Every bipartite field delivered a total photopic illuminance of 130 lx at the cornea. The full-field light condition was illuminated with the same blue LED, delivering the same CS = 0.60 (100 lx) at the cornea as each half-field. The temporal and nasal conditions were always set with respect to the participant’s dominant eye. (For interpretation of the references to colour in this figure legend, the reader is referred to the Web version of this article.)

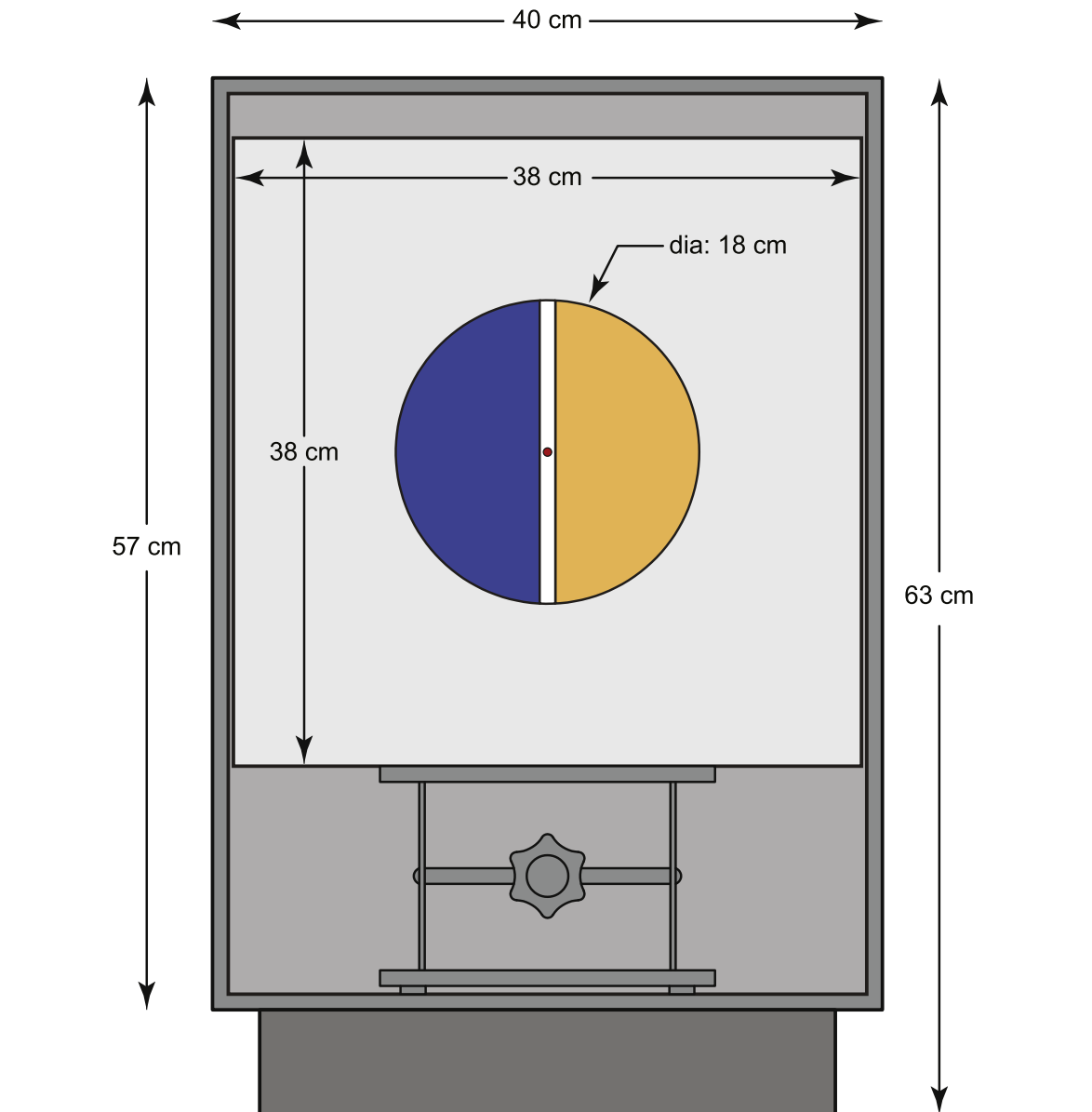


Fig. 2. The apparatus used for all experimental conditions, including the dark control. Illustrated is one of the four bipartite fields with the septum (white bar) dividing the blue and amber half-fields and the RGB LED fixation light at its centre. The other three bipartite fields were created by rotating the bipartite field around its centre axis, represented by the fixation light. The blue full-field was created by replacing the amber half-field with a second blue half-field and the two blue half-fields were calibrated to provide a combined CS of 0.60. The lights illuminating both half-fields were turned off for the dark control. The height of the apparatus was adjusted for each participant with a variable-height stand to maintain a level gaze of the apparatus. (For interpretation of the references to colour in this figure legend, the reader is referred to the Web version of this article.)

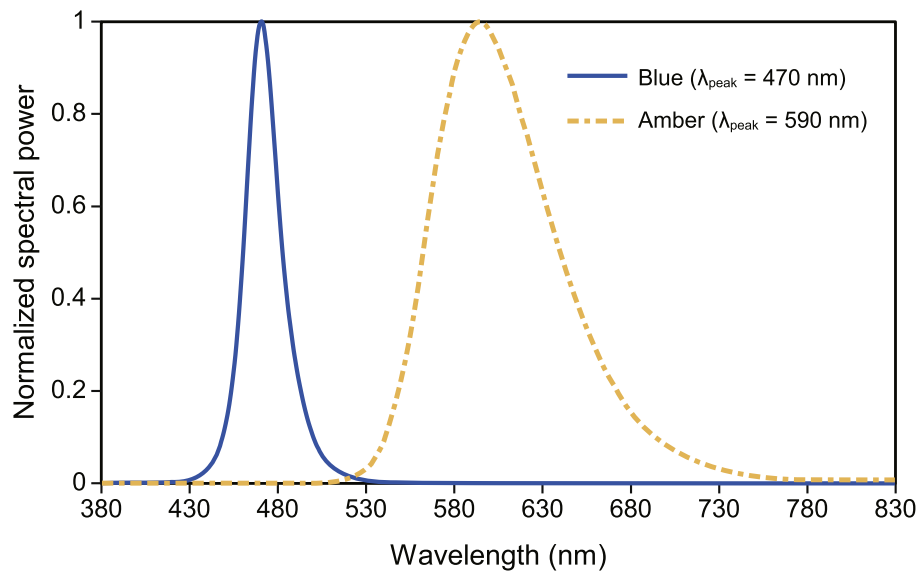


Fig. 3. Relative spectral power distributions for the blue and amber LED light sources. (For interpretation of the references to colour in this figure legend, the reader is referred to the Web version of this article.)

long dimension of the tube to see the fixation point. To ensure proper fixation throughout the protocol, participants had to perform a simple task. The fixation point usually appeared red (illuminance at the eye = 0.025 lx), but at occasional, random intervals the RGB LED would blink white a number of times (illuminance at the eye = 0.045 lx). Participants were required to record the number of blinks using a digital handheld counter. Throughout every 1-h exposure period, the number of blinks of the fixation point was randomly presented in 5-min cycles. In other words, all participants experienced exactly the same number of randomly generated, low-power blinks to ensure fixation was maintained. Values from the counter were noted and compared to actual blinks to verify participants complied with the fixation protocol. With very few exceptions, all participants accurately reported the number of blinks. To further ensure accurate delivery of the luminous stimulus, two experimenters monitored the behaviour of the participants and made spot measurements of the bipartite fields at the beginning and end of each session using an illuminance meter (Model X-91, Gigahertz-Optik, Haverhill Rd, Amesbury, MA, USA).

The photometric characteristics of the light stimuli presented to the participant's dominant eye are presented in Table 1; CL_A and CS were calculated following Rea and Figueiro (2018) and equivalent melanopic lux (EML) following Lucas et al. (2014). Table 2 shows the corresponding α -opic irradiances, calculated using the CIE S 026 α -opic Toolbox (v1.049). (Commission Internationale de l'Éclairage, 2018, 2020).

The brightness of the 40° luminous disc was expected to be high enough to fully constrict the participant's pupils. Pupil diameter was

Table 1
Photometric characteristics of the luminous stimuli.

Metric	Blue light source (Cree, XPEBBL-L1, $\lambda_{\text{peak}} = 470$ nm)	Amber light source (Lumileds LXML-PL01-0060, $\lambda_{\text{peak}} = 590$ nm)
Photopic illuminance (lx)	100.00	30.00
CL_A	1691.60	3.60
Melanopic equivalent (daylight) illuminance	733.68	1.85
CS	0.60	0

Abbreviations. CL_A : circadian light; CS: circadian stimulus; λ_{peak} : peak wavelength.

measured in a separate session with five volunteers using an entoptic pupilometer (Cogan, 1941), empirically demonstrating that participants had a fully constricted pupil (mean diameter = 2.1 mm) when exposed to all experimental conditions.

2.3. Study protocol

Participants arrived at the laboratory at 23:30 and remained in dim light (<5 lx at the eye) for 30 min, followed by a 60-min exposure to one of the six experimental conditions (Fig. 4).

Saliva samples were collected from each participant at three specific times over the course of each session. The first sample was taken at midnight, well after expected melatonin synthesis by the pineal and immediately before presentation of the experimental condition for that session. The second and third were collected 30 min and 60 min later during the experimental condition. At 01:05 participants were released from the laboratory.

Saliva samples (1 ml) were collected using the Salivette system (Sarstedt, Nümbrecht, DE). Participants chewed on a plain cotton cylinder for 1–2 min, which was then placed in a test tube. The tube containing the cotton cylinder was centrifuged for 5 min at 1000 g, and then immediately frozen (-20 °C). Every centrifuged sample for a participant was assayed in house in the same batch using melatonin radioimmunoassay kits (Catalog number 79-MELHU-R100, Direct Melatonin RIA, ALPCO, Salem, NH, USA). The Radioimmunoassay (RIA) is based on the competition principle. The specific antibody reacts with the corresponding antigen labelled with the I^{125} isotope. After separation of the bound from the free antigen by precipitation and centrifugation, the amount of the bound radioactivity of the precipitate was measured in a Gamma counter and results of samples were determined directly using the calibration curve. The minimum detection threshold for the melatonin radioimmunoassay kits was reported by the manufacturer to be 1 pg ml^{-1} . The sensitivity of the saliva sample assay was reported to be 0.3 pg ml^{-1} and the intra- and inter-assay coefficients of variability were 11.3% and 14.0%, respectively. During the experiment, the participants refrained from consuming any food and were allotted a 10-min window to drink water immediately following saliva sampling.

2.4. Data analysis

Insufficient amounts of saliva (<1 ml) were obtained from one

Table 2

The α -opic irradiances for all experimental conditions calculated using the CIE S 026 α -opic Toolbox (v1.049) (Commission Internationale de l'Éclairage, 2020).

Stimulus lights	S-cone-opic irradiance W m^{-2}	M-cone-opic irradiance W m^{-2}	L-cone-opic irradiance W m^{-2}	Rhodopic irradiance W m^{-2}	Melanopic irradiance W m^{-2}
Blue light source (Cree, XPEBBL-L1, $\lambda_{\text{peak}} = 470 \text{ nm}$)	0.61	0.36	0.21	0.81	0.97
Amber light source (Lumileds LXML-PL01-0060, $\lambda_{\text{peak}} = 590 \text{ nm}$)	0	0.03	0.05	0.01	0

Abbreviation. λ_{peak} : peak wavelength.

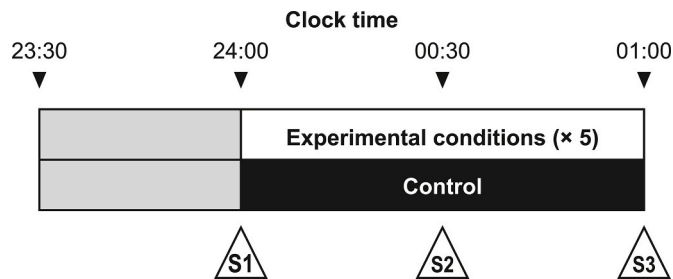


Fig. 4. The experimental protocol for each of the six counterbalanced sessions. The grey bars correspond to the initial dim light exposure. The white bar designates the presentation of one of the five experimental lighting conditions or the dark control (black bar). S1–3 indicate when saliva samples were collected.

participant for the “nasal” luminous stimulus condition (S2 and S3, Fig. 4); otherwise all other saliva samples were analysed. For each session, melatonin concentrations for S2 and S3 were first normalized to S1, and the melatonin suppression at both times was then calculated using Equation (1).

$$\text{Percent suppression} = 1 - \left(\frac{M_n}{M_d} \right) \times 100 \quad (1)$$

where M_n is the normalized melatonin concentration at each time on the respective intervention nights and M_d is the normalized melatonin concentration at each corresponding time on the dark control night.

Preliminary statistical analysis detected melatonin suppression values for two participants under the nasal condition (S3) as far outliers (Criterion: $y > Q_3 + 3.0 \times \text{IQR}$, or, $y < Q_1 - 3.0 \times \text{IQR}$ —where y is the data point, Q_1 is the lower quartile, Q_3 is the upper quartile, IQR is the inter-quartile range or $Q_3 - Q_1$) and those two data points have been excluded from the primary statistical analysis.

Given the two missing saliva samples and the two excluded outlier data, a primary analysis of variance (ANOVA) was performed using a linear mixed effect model with the five lighting distribution conditions (Fig. 1) and the two exposure durations (S2 and S3, Fig. 4) as levels of the two within-subject independent variables and melatonin suppression as the dependent variable. Baseline melatonin levels (S1, Fig. 4) across the six experimental conditions (including the dark control) were also subjected to a second mixed model ANOVA to determine whether melatonin concentrations were statistically the same at the start of the experiment. The ANOVAs were performed with SPSS statistical software (SPSS version 26, IBM, Armonk, NY, USA). The test results were considered statistically significant if the probability of a Type I error (P) was < 0.05 . Mauchly’s test indicated that the assumption of sphericity was not violated ($\chi^2(9) = 15.53$, $P = 0.08$) while performing the ANOVA. *Post hoc* multiple pairwise comparisons were performed with Bonferroni corrections.

3. Results

3.1. Baseline melatonin levels

The second ANOVA revealed that the absolute baseline melatonin

levels recorded at the beginning of each study night (S1) were not significantly different across the six experimental conditions (mean melatonin concentration = 8.54 pg ml^{-1} ; $F_{5,72} = 0.36$, $P = 0.88$) (Table 3). It is important that the melatonin concentrations at S1 were above sampling noise levels because subsequent melatonin concentrations at S2 and S3 were normalized to these baseline levels to calculate melatonin suppression (Equation (1); Supplementary Table S1). It should be noted that we were not concerned with how light affects circadian phase but, rather, the aim of the study was to accurately estimate the magnitude of light-induced melatonin suppression. Therefore, as long as melatonin was being synthesized by the pineal gland and saliva sampling time was not confounded with systematic variations in the experimental conditions, our results would be consistent with the goal of the study. Since participants were following regular bed- and wake-time schedules, the times of collecting saliva samples were after their bedtimes and were constant for all conditions. Moreover, their melatonin levels prior to energizing the lights (S1) were always above the sampling threshold for detection (again, the mean concentration was 8.54 pg ml^{-1}), so any slight variation in the time that melatonin synthesis began among participants can be considered as a random, extraneous variable and not one confounded with the experimental conditions. Thus, the inferential statistics associated with light-induced nocturnal melatonin suppression were not compromised.

3.2. Effect of lighting characteristics on melatonin suppression

The primary ANOVA, performed on S2 and S3 melatonin levels normalized to the respective S1 melatonin levels for each participant (excluding the outliers) and re-normalized relative to the dark night melatonin levels (based upon raw data from Supplementary Table 1), revealed a significant main effect of light exposure duration ($F_{1,131} = 9.59$, $P < 0.01$), wherein, as expected, greater melatonin suppression was observed for longer durations during the participants’ early biological night.

The primary ANOVA also revealed a significant main effect of lighting distribution on melatonin suppression ($F_{4,131} = 4.19$, $p < 0.01$; Fig. 5). No statistically significant interaction between distribution and duration was identified ($F_{4,131} = 0.98$, $p = 0.42$).

Because all four of the excluded data came from the nasal stimulus condition, a supplementary ANOVA was performed to ensure the results were not inadvertently biased in the primary ANOVA. Data for all experimental conditions from three participants (two participants with statistical outliers at S3 and one participant missing two saliva samples at S2 and S3) were excluded. This ANOVA led to the same statistical inferences, namely, exposure durations ($F_{1,108} = 10.19$, $p < 0.01$) and lighting distribution ($F_{4,108} = 5.27$, $p < 0.01$) were statistically significant, but not the interaction ($F_{4,108} = 0.72$, $p = 0.60$). *Post hoc* analysis,

Table 3
Mean absolute baseline salivary melatonin levels at S1.

Experimental condition	Dim light	Nasal	Temporal	Superior	Inferior	Full-field
Mean (SD) melatonin level (pg ml^{-1})	8.7 (7.2)	8.3 (5.5)	8.7 (7.2)	8.7 (7.0)	8.4 (6.3)	7.9 (5.4)

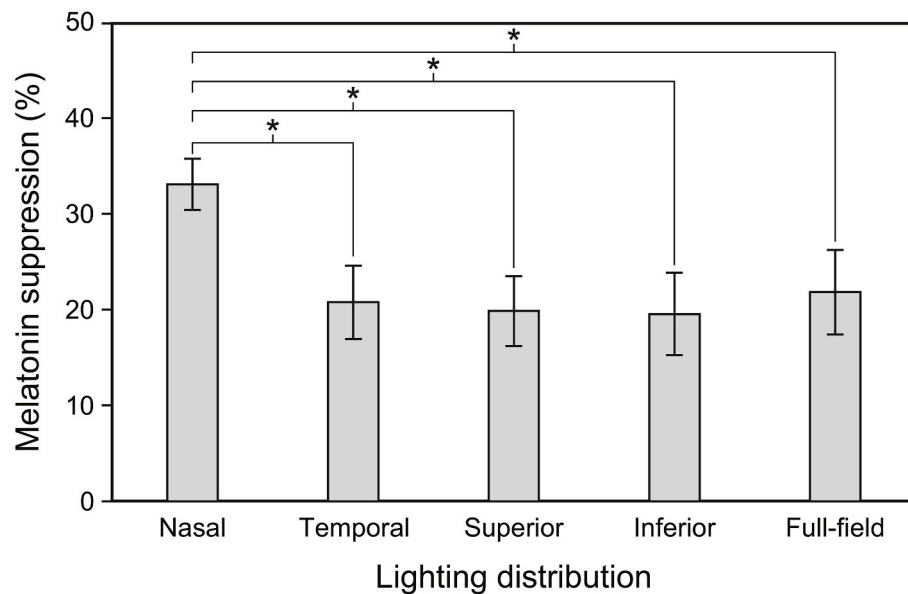


Fig. 5. Main effect of lighting distribution on nocturnal melatonin suppression. The error bars represent SEM, * represents $p < 0.05$.

following both the primary and supplementary ANOVAs, revealed that melatonin suppression following the nasal exposure was significantly different than all other conditions.

Specifically, as can be seen in Fig. 5, the greatest melatonin suppression was associated with light exposure in the nasal hemi-field. The other three hemi-fields as well as the full-field exposure resulted in similar suppression levels. *Post hoc* pairwise comparisons with Bonferroni correction supported that inference, namely the average melatonin suppression obtained following illumination of the nasal retina (mean = 33.1% [SEM 2.7]) was significantly greater ($P < 0.05$) than the average melatonin suppression levels recorded for the temporal retina (mean = 20.8% [SEM 3.8]), superior retina (mean = 19.8% [SEM 3.6]), inferior retina (mean = 19.5% [SEM 4.3]), and for the full-field exposure (mean = 21.8% [SEM 4.4]). Further, melatonin suppression for these other four conditions were not statistically different ($p > 0.05$).

4. Discussion

By controlling the distribution of light entering the eye, the present study was able to explore the inconsistencies in the psychophysical literature regarding differential spatial sensitivity of the human retina to circadian-effective light. The present results support the conclusions reached by R uger et al. (2005) and by Visser et al. (1999) that the nasal hemi-field of the human retina is more sensitive to circadian-effective light exposures than the temporal, superior, and inferior retinal hemi-fields, all three of which were equally sensitive. Our findings are indirectly and partially supported by the study of post-illumination pupillary reflex (PIPR) to blue light exposure by Lei et al. (2015), who showed that the inferior and the superior retinal hemi-fields were equally effective at producing longer-term pupil constriction.

Naturally one looks to the neuroanatomy for convergence with these psychophysical results, expecting perhaps that there would be a greater density of M1 ipRGC cell-bodies in the nasal retina. Although there are limited neuroanatomical data available, the highest density of M1 ipRGCs cell-bodies appears to be similar to that of other retinal ganglion cells, forming a high-density concentric annulus around the fovea (Hannibal et al., 2017; Nasir-Ahmad et al., 2019). Extending radially from the fovea, there does not appear to be any significant differential change in M1 ipRGC cell-body density, although there does appear to be a higher density of M2 ipRGC cell-bodies, with projections mainly to the lateral geniculate nucleus (LGN), in the nasal hemi-field than in the

temporal hemi-field of the retina (Nasir-Ahmad et al., 2019). In other words, there is no evidence that the nasal retina might be more sensitive than the temporal retina to circadian-effective light because of differences in M1 ipRGC cell-body densities. In contrast, the distribution of ipRGC axons forming the RHT are not radially symmetric. Rather, as part of the papillomacular bundle, they would provide an asymmetric, greater sensitivity to circadian effective light in the near nasal field ($<20^\circ$).

As a further consideration, while the M1 ipRGCs are central to circadian phototransduction (Dacey et al., 2005), they are not the only participating neurons. Shunting inhibition from rods neural signals via AII amacrine neurons was postulated in the 2005 (Rea et al., 2005) and 2021 (Rea et al., 2021a, 2021b) models of circadian phototransduction to control the M1 ipRGC threshold to blue light exposure like that used in the present study. Similar to the relative densities of ipRGCs, rod densities are not very different in the four retinal hemi-fields (Curcio et al., 1990; Packer et al., 1989). However, the rod-to-cone ratio is much lower in the nasal hemi-field relative to the temporal, superior, and inferior hemi-fields (Curcio et al., 1990). Since cones suppress rod-generated neural responses through the AII/A17 complex (Graham and Wong, 1995) a lower rod-to-cone ratio could mean that the threshold for deactivating shunting inhibition is lower, thus increasing the relative sensitivity of the nasal hemi-field to circadian-effective light.

To control the distribution of light entering the eye, the luminous stimuli were viewed monocularly. Naturally, there would be an expected reduction in neural input to the SCN relative to viewing the luminous stimuli binocularly. Quite surprisingly, monocular viewing does not reduce the effective stimulus by 50% but, rather, by approximately 90% (Spitschan and Cajochen, 2019). The full-field stimulus condition employed in the present study was calibrated to produce a binocular circadian stimulus (CS) of 0.60, corresponding to an expected 60% suppression of nocturnal melatonin after a 1-h exposure. Based upon the estimates from Spitschan and Cajochen (2019), a 90% reduction in effective light stimulus would translate to a binocular CS = 0.21, with an expected suppression of melatonin of 21% after 1 h of light exposure. The present results showed a 24% suppression of melatonin after 1 h for the full-field stimulus condition which, following a two-tailed, one sample *t*-test, was not significantly different than a 21% reduction ($t_{15} = 0.48$, $p = 0.64$).

It will be recalled that all of the luminous fields, not just the full-field, were calibrated to produce a binocular CS = 0.60. This being the case, it

would be reasonable to assume that the average suppression of melatonin for the four half-fields should be equivalent to the full field set to the same circadian stimulus level (i.e., a binocular CS = 0.60). In other words, assuming a simple additive model for suppression, the net full-field stimulus (delivering same irradiance as each half-field condition) can be broken down into four stimuli with 25% relative strength targeting all four retinal hemi-fields. For the 1-h exposure duration, a corresponding drop of 75% in response for the nasal, temporal, superior, and inferior conditions yields 1-h melatonin suppression values of 10.1%, 6.7%, 4.9%, and 5.7%, respectively, adding up to a net suppression of 27.4%. This net suppression, or the average 1-h suppression across the four hemi-fields, was not significantly different than 24% suppression for the full-field exposure for the same level of CS according to a two-tailed one sample *t*-test ($t_{15} = 0.50$, $p = 0.62$). This average suppression was, however, statistically different from the monocular-adjusted CS = 0.21 based upon the estimate from (Spitschan and Cajochen, 2019) ($t_{60} = 2.41$, $p < 0.05$; two-tailed). This discrepancy perhaps suggests that the reduction in effective stimulus level from binocular to monocular is not quite 90% as Spitschan & Cajochen estimated, but closer to 87% or 85%, which would correspond to a CS = 0.24 or CS = 0.27, respectively. The 5% discrepancy in these estimates (85–90%) is, in our opinion, small, but naturally, additional research providing a more exact estimates of binocular versus monocular exposures would be useful.

Light therapy is often used to correct circadian disruption (Blume et al., 2019; Faulkner et al., 2019). Practically speaking, light therapy boxes need to be displaced from the direction of gaze so that the persons receiving the therapy can continue to be engaged in visual tasks, like reading, that require foveal vision. From the present results, light therapy aimed at correcting circadian disruption would be most effective if two light boxes were placed to the left and to the right of the direction of gaze rather than directly above and below. At these two locations, each light box would be focused on the more sensitive nasal retina of each eye. Using just one peripheral light box might reduce the effective light stimulus substantially (85–90%) if it were only imaged on the retina of one eye. Two, equally luminous light boxes, laterally displaced from the direction of gaze and imaged on the nasal retina of each eye, would ensure delivery of a prescribed CS level.

The same principles would apply for architectural lighting. Light emanating from the ceiling, which is most common, will be much less effective than light reaching the eyes from both sides. Two light sources mounted or placed adjacent to the sides of a computer monitor would be very effective for maintaining circadian entrainment of workers in commercial spaces. And by splitting the circadian-effective light in two, there is less likelihood of discomfort glare (Bullough et al., 2008).

Stimulation of the nasal retina produced an approximately 15% greater response to light stimulation than the other three quadrants. In terms of the magnitude of this difference, it should be understood that a difference of 15% relates to the outcome, not the input to system. A 15% difference in outcome represents a greater than 100% difference in light input due to the non-linear operating characteristic of circadian phototransduction. For example, 225 lx for a cool-white light source (6500 K) will suppress nocturnal melatonin by 30% after 1-h exposure (see computational formulations by Rea et al. (2021a)). Only 91 lx is needed to suppress melatonin by 15% after 1-h exposure, a difference in CS of 15% but a difference of 147% in flux density at the eyes. We believe, therefore, particularly considering energy use, that a factor of 2 × in light intensity is significant.

The present results also suggest an interesting approach to maintaining melatonin levels at night among shift workers. Monocular light exposures are disproportionately less effective for suppressing melatonin than binocular exposures. Whereas it might be possible to work with one eye occluded during night-shift work, it seems much more practical and comfortable to maintain binocular vision, but cover one eye with a blue-blocking filter. This would effectively make one eye “blind” to circadian-effective light while providing good visibility to both eyes. This practical

notion should be explored experimentally in the future.

Finally, a few limitations to the study are worth noting. First, we did not monitor or control participants’ photic history; daily light exposures over the course of the study were presumed constant because all participants kept regular schedules. We acknowledge that we did not specifically assess the participants’ circadian phase (e.g., dim light melatonin onset), but because sampling times were constant for all experimental conditions and because melatonin was being synthesized during sampling (mean = 8.54 pg ml⁻¹), the exact time of melatonin synthesis onset would not be confounded with the experimental conditions and therefore would not compromise the validity of the inferential statistics. To analytically address variance associated with changes to individual circadian sensitivity on a study night, absolute melatonin levels recorded post energizing the light fixtures (S2, S3) were always normalized to the baseline melatonin levels (S1), which have been found to be statistically similar across all experimental conditions (or all study nights).

Second, all the participants were exposed to only one type of luminous stimulus, namely, prolonged exposure to one level of a diffuse, narrow-band light source (binocular CS = 0.60 from blue LEDs); potential interactions among stimulus variables could not be assessed. Third, the adult participants recruited for the study represented a wide age distribution (23–54 years of age). However, while absolute differences in relative sensitivity for the four hemi-fields may occur with a different set of participants, it is unlikely that the inference for greater sensitivity to circadian-effective light in the nasal retina is invalid because this was a within-subjects study. Any individual difference in, for example, sensitivity to short-wavelength (blue) light, is incorporated in all of the experimental conditions. Lastly, even though counter-balanced presentation of the experimental conditions to the participants was organized in terms of groups and not individuals, each participant was initially randomized to that specific group.

Funding

This work was supported by the Jim H. McClung Lighting Research Foundation (all authors) and by the NIH Training Grant (Rohan Nagare, grant number 5T32AG057464).

CRediT authorship contribution statement

Mark S. Rea: Conceptualization, Methodology, Writing – original draft, Visualization. **Rohan Nagare:** Formal analysis, Investigation, Data curation, Writing – original draft. **Mariana G. Figueiro:** Methodology, Validation, Resources, Supervision, Writing – review & editing, Project administration, Funding acquisition.

Declaration of competing interest

The author(s) have no potential conflicts of interest with respect to the research, authorship, and/or publication of this article.

Acknowledgments

The authors would like to acknowledge Andrew Bierman, John Bullough, Jean Paul Freyssinier, Charles Jarboe, Sharon Lesage, Martin Overington, David Pedler, and Barbara Plitnick for their technical and editorial assistance.

Appendix A. Supplementary data

Supplementary data to this article can be found online at <https://doi.org/10.1016/j.nbscr.2021.100066>.

References

- Baver, S.B., Pickard, G.E., Sollars, P.J., Pickard, G.E., 2008. Two types of melanopsin retinal ganglion cell differentially innervate the hypothalamic suprachiasmatic nucleus and the olivary pretectal nucleus. *Eur. J. Neurosci.* 27 (7), 1763–1770. <https://doi.org/10.1111/j.1460-9568.2008.06149.x>.
- Blume, C., Garbaza, C., Spitschan, M., 2019. Effects of light on human circadian rhythms, sleep and mood. *Somnologie* 23 (3), 147–156. <https://doi.org/10.1007/s11818-019-00215-x>.
- Bullough, J.D., Brons, J.A., Qi, R., Rea, M.S., 2008. Predicting discomfort glare from outdoor lighting installations. *Light. Res. Technol.* 40 (3), 225–242. <https://doi.org/10.1177/1477153508094048>.
- Burgess, H.J., Fogg, L.F., 2008. Individual differences in the amount and timing of salivary melatonin secretion. *PLoS One* 3 (8), e3055. <https://doi.org/10.1371/journal.pone.0003055>.
- Cogan, D.G., 1941. A simplified entoptic pupillometer. *Am. J. Ophthalmol.* 24 (12), 1431–1433. [https://doi.org/10.1016/S0002-9394\(14\)77456-2](https://doi.org/10.1016/S0002-9394(14)77456-2).
- Commission Internationale de l'Éclairage, 2018. *CIE System for Metrology of Optical Radiation for ipRGC-Influenced Responses to Light*, CIE S 026/E:2018. Commission Internationale de l'Éclairage. <http://cie.co.at/publications/cie-system-metrology-optical-radiation-iprgc-influenced-responses-light-0>.
- Commission Internationale de l'Éclairage, 2020. *The α -opic Toolbox* (v1.049, 2020/03/26. Commission Internationale de l'Éclairage, Vienna. <https://bit.ly/33YM9Rh>.
- Curcio, C.A., Sloan, K.R., Kalina, R.E., Hendrickson, A.E., 1990. Human photoreceptor topography. *J. Comp. Neurol.* 292 (4), 497–523. <https://doi.org/10.1002/cne.902920402>.
- Dacey, D., Liao, H.-W., Peterson, B., Robinson, F., Smith, V.C., Pokorny, J., Yau, K.-W., Gamlin, P., 2005. Melanopsin-expressing ganglion cells in primate retina signal colour and irradiance and project to the LGN. *Nature* 433, 749–754. <https://doi.org/10.1038/nature03387>.
- Esquiva, G., Lax, P., Perez-Santonja, J.J., Garcia-Fernandez, J.M., Cuenca, N., 2017. Loss of melanopsin-expressing ganglion cell subtypes and dendritic degeneration in the aging human retina. *Front. Aging Neurosci.* 9, 79. <https://doi.org/10.3389/fnagi.2017.00079>.
- Faulkner, S.M., Bee, P.E., Meyer, N., Dijk, D.-J., Drake, R.J., 2019. Light therapies to improve sleep in intrinsic circadian rhythm sleep disorders and neuro-psychiatric illness: a systematic review and meta-analysis. *Sleep Med. Rev.* 46, 108–123. <https://doi.org/10.1016/j.smrv.2019.04.012>.
- Fernandez, D.C., Chang, Y.-T., Hattar, S., Chen, S.-K., 2016. Architecture of retinal projections to the central circadian pacemaker. *Proc. Natl. Acad. Sci. U.S.A.* 113 (21), 6047–6052. <https://doi.org/10.1073/pnas.1523629113>.
- Gaddy, J.R., Edelson, M., Stewart, K., Brainard, G.C., Rollag, M.D., 1992. Possible retinal spatial summation in melatonin suppression. In: Holick, M.F., Klingman, A.M. (Eds.), *Biologic Effects of Light*. Walter de Gruyter, New York, pp. 196–204.
- Glickman, G., Hanifin, J.P., Rollag, M.D., Wang, J., Cooper, H., Brainard, G.C., 2003. Inferior retinal light exposure is more effective than superior retinal exposure in suppressing melatonin in humans. *J. Biol. Rhythm.* 18 (1), 71–79. <https://doi.org/10.1177/0748730402239678>.
- Graham, D.M., Wong, K.Y., 1995. Melanopsin-expressing, intrinsically photosensitive retinal ganglion cells (ipRGCs). In: Kolb, H., Fernandez, E., Nelson, R. (Eds.), *Webvision: the Organization of the Retina and Visual System*. University of Utah Health Sciences Center. <https://webvision.med.utah.edu/book/part-ii-anatomy-and-physiology-of-the-retina/melanopsin-expressing-intrinsically-photosensitive-retinal-ganglion-cells/>.
- Hannibal, J., Christiansen, A.T., Heegaard, S., Fahrenkrug, J., Kiilgaard, J.F., 2017. Melanopsin expressing human retinal ganglion cells: subtypes, distribution, and intraretinal connectivity. *J. Comp. Neurol.* 525 (8), 1934–1961. <https://doi.org/10.1002/cne.24181>.
- Ishihara, S., 1960. In: *Tests for Colour-Blindness*, 15 ed. H. K. Lewis, London.
- Kolb, H., Nelson, R., Ahnelt, P., Ortuño-Lizarán, I., Cuenca, N., 2020. The architecture of the human fovea. In: Kolb, H., Nelson, R., Fernandez, E. (Eds.), *Webvision: the Organization of the Retina and Visual System*, vol. 2020. University of Utah Health Sciences Center. <https://www.ncbi.nlm.nih.gov/books/NBK554706/>.
- Kooijman, A.C., 1983. Light distribution on the retina of a wide-angle theoretical eye. *J. Opt. Soc. Am.* 73 (11), 1544–1550. <https://doi.org/10.1364/josa.73.001544>.
- Kriegsfeld, L.J., Leak, R.K., Yackulic, C.B., LeSauter, J., Silver, R., 2004. Organization of suprachiasmatic nucleus projections in Syrian hamsters (*Mesocricetus auratus*): an anterograde and retrograde analysis. *J. Comp. Neurol.* 468 (3), 361–379. <https://doi.org/10.1002/cne.10995>.
- La Morgia, C., Ross-Cisneros, F.N., Sadun, A.A., Hannibal, J., Munarini, A., Mantovani, V., Barboni, P., Cantalupo, G., Tozer, K.R., Sancisi, E., Salomao, S.R., Moraes, M.N., Moraes-Filho, M.N., Heegaard, S., Milea, D., Kjer, P., Montagna, P., Carelli, V., 2010. Melanopsin retinal ganglion cells are resistant to neurodegeneration in mitochondrial optic neuropathies. *Brain* 133 (Pt 8), 2426–2438. <https://doi.org/10.1093/brain/awq155>.
- Lasko, T., Kripke, D., Elliot, J., 1999. Melatonin suppression by illumination of upper and lower visual fields. *J. Biol. Rhythm.* 14 (2), 122–125. <https://doi.org/10.1177/074873099129000506>.
- Lei, S., Goltz, H.C., Chandrakumar, M., Wong, A.M., 2015. Test-retest reliability of hemifield, central-field, and full-field chromatic pupillometry for assessing the function of melanopsin-containing retinal ganglion cells. *Invest. Ophthalmol. Vis. Sci.* 56 (2), 1267–1273. <https://doi.org/10.1167/iov.14-15945>.
- Lucas, R.J., Peirson, S.N., Berson, D.M., Brown, T.M., Cooper, H.M., Czeisler, C.A., Figueiro, M.G., Gamlin, P.D., Lockley, S.W., O'Hagan, J.B., Price, L.L., Provencio, I., Skene, D.J., Brainard, G.C., 2014. Measuring and using light in the melanopsin age. *Trends Neurosci.* 37 (1), 1–9. <https://doi.org/10.1016/j.tins.2013.10.004>.
- Nasir-Ahmad, S., Lee, S.C.S., Martin, P.R., Grünert, U., 2019. Melanopsin-expressing ganglion cells in human retina: morphology, distribution, and synaptic connections. *J. Comp. Neurol.* 527 (1), 312–327. <https://doi.org/10.1002/cne.24176>.
- Packer, O., Hendrickson, A.E., Curcio, C.A., 1989. Photoreceptor topography of the retina in the adult pigtail macaque (*Macaca nemestrina*). *J. Comp. Neurol.* 288 (1), 165–183. <https://doi.org/10.1002/cne.902880113>.
- Pflibsen, K.P., Pomerantzeff, O., Ross, R.N., 1988. Retinal illuminance using a wide-angle model of the eye. *J. Opt. Soc. Am. A* 5 (1), 146–150. <https://doi.org/10.1364/josaa.5.000146>.
- Portaluppi, F., Smolensky, M.H., Touitou, Y., 2010. Ethics and methods for biological rhythm research on animals and human beings. *Chronobiol. Int.* 27 (9–10), 1911–1929. <https://doi.org/10.3109/07420528.2010.516381>.
- Rea, M.S., Figueiro, M.G., 2018. Light as a circadian stimulus for architectural lighting. *Light. Res. Technol.* 50 (4), 497–510. <https://doi.org/10.1177/1477153516682368>.
- Rea, M.S., Figueiro, M.G., Bullough, J.D., Bierman, A., 2005. A model of phototransduction by the human circadian system. *Brain Res. Rev.* 50 (2), 213–228. <https://doi.org/10.1016/j.brainresrev.2005.07.002>.
- Rea, M.S., Nagare, R., Figueiro, M.G., 2021a. Modeling circadian phototransduction: quantitative predictions of psychophysical data. *Front. Neurosci.* 15, 44. <https://doi.org/10.3389/fnins.2021.615322>.
- Rea, M.S., Nagare, R., Figueiro, M.G., 2021b. Modeling circadian phototransduction: retinal neurophysiology and neuroanatomy. *Front. Neurosci.* 14, 1467. <https://doi.org/10.3389/fnins.2020.615305>.
- Roenneberg, T., Wirz-Justice, A., Mellow, M., 2003. Life between clocks: daily temporal patterns of human chronotypes. *J. Biol. Rhythm.* 18 (1), 80–90. <https://doi.org/10.1177/0748730402239679>.
- Rosenwasser, A.M., Turek, F.W., 2015. Neurobiology of circadian rhythm regulation. *Sleep Med. Clin.* 10 (4), 403–412. <https://doi.org/10.1016/j.jsmc.2015.08.003>.
- Rüger, M., Gordijn, M.C., Beersma, D.G., de Vries, B., Daan, S., 2005. Nasal versus temporal illumination of the human retina: effects on core body temperature, melatonin, and circadian phase. *J. Biol. Rhythm.* 20 (1), 60–70. <https://doi.org/10.1177/0748730404270539>.
- Spitschan, M., Cajochen, C., 2019. Binocular facilitation in light-mediated melatonin suppression? *J. Pineal Res.* 67 (4), e12602. <https://doi.org/10.1111/jpi.12602>.
- Van Derlofske, J., Bierman, A., Rea, M.S., Ramanath, J., Bullough, J.D., 2002. Design and optimization of a retinal flux density meter. *Meas. Sci. Technol.* 13 (6), 821–828. <https://doi.org/10.1088/0957-0233/13/6/301>.
- Visser, E.K., Beersma, D.G., Daan, S., 1999. Melatonin suppression by light in humans is maximal when the nasal part of the retina is illuminated. *J. Biol. Rhythm.* 14 (2), 116–121. <https://doi.org/10.1177/074873099129000498>.